Microchemical Journal 181 (2022) 107820

Contents lists available at ScienceDirect

Microchemical Journal

journal homepage: www.elsevier.com/locate/microc

Electrochemical chiral sensor based on molecularly imprinted polymer for determination of (1S,2S)-pseudoephedrine in dosage forms and biological sample

Leyla Karadurmus [a,b], Goksu Ozcelikay [a], Canan Armutcu [c], Sibel A. Ozkan [a,*]

[a] Ankara University, Faculty of Pharmacy, Department of Analytical Chemistry, Ankara, Turkey
[b] Adıyaman University, Faculty of Pharmacy, Department of Analytical Chemistry, Adıyaman, Turkey
[c] Hacettepe University, Faculty of Science, Department of Chemistry, Ankara, Turkey

ARTICLE INFO

Keywords:
Molecularly imprinted polymers
Pseudoephedrine enantiomers
Glassy carbon electrode
Voltammetry
Ortho-phenylenediamine

ABSTRACT

In this study, simple, eco-friendly, highly sensitive, and selective molecularly imprinted polymer-based electrochemical chiral (MIEC) sensors were fabricated for the detection of Pseudoephedrine (PSDO) enantiomers. The sensitive and selective platform was prepared by in-situ electropolymerization of o-phenylenediamine (o-PD) on a glass carbon electrode in the presence of the template molecule, PSDO. The MIP modified sensor surface was characterized with Raman spectrometer, contact angle measurements, and scanning electron microscopy (SEM) to confirm successful preparation. Furthermore, cyclic voltammetry and electrochemical impedance spectroscopy were applied to test the electrochemical property of the sensor. Under the optimal conditions, the linear response of (1S,2S)-PSDO was obtained in the range of $1x10^{-15}$ – $1x10^{-14}$ M in the commercial human serum samples and effervescent tablets. Moreover, the high recovery data were obtained as 100.5 % and 100.4 % in pharmaceutical dosage forms and commercial human serum samples by the proposed (1S,2S)-PSDO@MIP/GCE sensor, respectively. The developed (1S,2S)-PSDO@MIP/GCE sensor has an excellent selectivity towards (1R,2R)-PSDO with an imprinting factor of 4.97.

1. Introduction

Pseudoephedrine (PSDO) is a diastereomer of ephedrine with sympathomimetic properties and member of the class of amphetamine and phenylethanolamines that is mainly reduced into methamphetamine or oxidized into methcathinone (Scheme 1) [1].

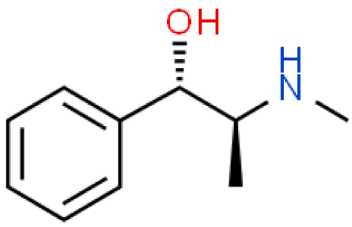
Pseudoephedrine causes vasoconstriction of blood vessels, including the nasal mucosa, a reduction in blood content, and shrinking swollen of the mucosa [2,3]. PSDO are generally taken with antipyretic drugs to treat cold and flu and with antihistamines to reduce allergic reactions [4]. PSDO are known as stimulants [5] that are widely abused in competitive sports. PSDO has included alkaloid derivatives. Moreover, PSDO is on the list of prohibited substances by the International Olympic Committee and sports federations because of its addictive properties [6].

For this reason, the rapid and sensitive analytical determination of PSDO has a very important place in the field of sports [7]. The declaration of "ephedrine-free" products is crucial in the analysis of different product formulations. The PSDO is became a banned substance when exceeded the threshold of 25 μg/mL in athlete urinary samples [8,9] Up to now, many analytical approaches have been presented for quantifying the analysis of PSDO with electrochemical methods [10–15], spectroscopy[16], HPLC[17], GC[18,19], and capillary electrophoresis (CE) [20]. Compared with traditional techniques, electrochemical methods are known as one of the most used techniques because of their green-chemistry properties, low consumption analyte, short time-period, user-friendly, acquired low detection, and wide linear range. CV and EIS are generally preferred to enlighten the characterization of developed sensors in the presence of Ferri/Ferrocyanide redox couple as a redox marker. DPV is widely utilized for the determination of analytes in supporting electrolytes, pharmaceuticals dosage form, and biological samples [21]. The indirect electrochemical detection of PSDO was allowed by the change of ferrocene group redox properties upon the exposure to PSDO. It was decided to use an indirect sensing method based on an electroactive probe ion because of obtaining the greater low limit of detection.

Until now, various electrochemical sensors have been developed for

* Corresponding author.
E-mail address: ozkan@pharmacy.ankara.edu.tr (S.A. Ozkan).

https://doi.org/10.1016/j.microc.2022.107820
Received 31 January 2022; Received in revised form 30 May 2022; Accepted 25 July 2022
Available online 29 July 2022
0026-265X/© 2022 Elsevier B.V. All rights reserved.



Scheme 1. The chemical structure of PSDO.

the determination of PSDO. In 1996, ephedrine, PSDO and norephedrine were analyzed by Gonzalez-Lomba J.R.'s research group [13]. LOD was reported as approximately 0.5 $mgmL^{-1}$ for each. In 2012, Ahmar H. et al. developed the carboxyl functionalized multi-walled carbon nanotubes modified electrochemical sensor to determine ephedrine and PSDO in pharmaceutical dosage form and urine sample. The adsorptive stripping voltammetry was performed, and the limit of detection (LOD) was found as 0.75 μM and 0.82 μM for ephedrine and PSDO, respectively [14]. Hameed A. presented that a core–shell structured Ni–Co@Pt/C nanocomposite was synthesized and applied as electrochemical modification agents [15]. The developed nanosensor was used for the determination of PSDO. The detection limit of 4.17 μM was obtained for PSDO. In these articles, the selectivity and sensitivity are not sufficient for determining PSDO in biological samples. Therefore, this situation has increased the importance of MIP-based electrochemical sensors. Furthermore, this work is the first attempt to use MIP-based electrochemical sensor to determine PSDO.

MIP-based electrochemical sensors have a superiority comparison with traditional electrochemical sensors [22–24]. Molecularly imprinted techniques are very useful for determining various analytes, from large to small structures [22–24]. The MIPs are formed in the presence of template molecule, monomer, cross-linker (if needed), and initiator (if needed). The polymerization process is mainly designed with four methods: thermal polymerization, photopolymerization, electropolymerization, and sol–gel polymerization [25].

Polymeric matrices are formed with electropolymerization technique on electrode surface to obtain MIP-based electrochemical sensors by CV. Cycle number and a scan rate of the process determine polymer thickness. The monomer has a key role in forming the polymeric matrix. The o-phenylenediamine (*o*-PD), methacrylic acid, pyrrole, phenol, aniline, and derivates are widely referred to as the most used monomers in literature [26].

The made-tailor cavity of the analyte is created on a polymeric matrix. Then, the analyte is indwelled to prepare specific cavities by means of interaction consisting of hydrophobic bonding, hydrogen bonding, electrostatic interactions, and Van der Waals forces [27]. One of the advantages of MIP is that the cavity is adjustable according to the molecule's shape, size, and charge distribution. Therefore, the MIP-based sensor is the best analytical method with its high specificity and selectivity properties.

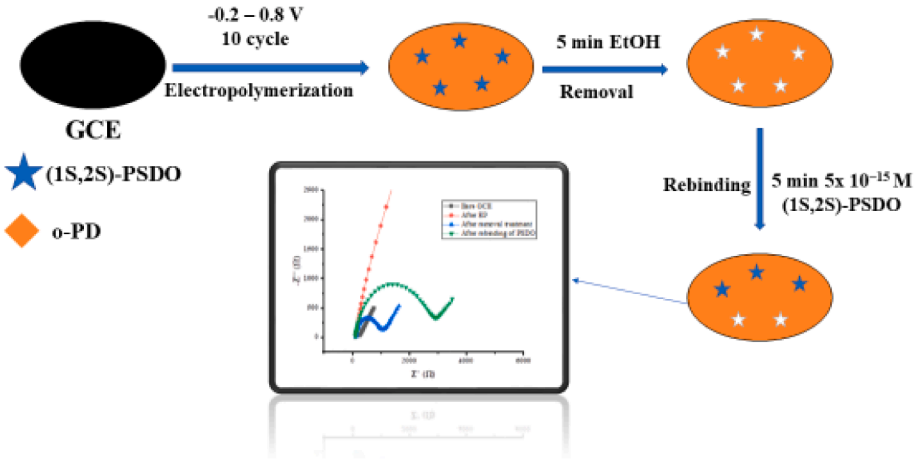
This work aims to develop the first sensitive and selective MIP-based electrochemical chiral sensor for the selective and sensitive detection of (1S,2S)-PSDO in commercial biological samples and pharmaceutical dosage form. (1S,2S)-PSDO templated chiral MIP sensor was electrochemically synthesized on a GCE by electropolymerization of o-PD monomer in the presence of (1S,2S)-PSDO. The MIP-based electrochemical chiral sensor showed low detection time, excellent sensitivity, high selectivity, and short analysis time for the electrochemical detection of the (1S,2S)-PSDO.

2. Experimental

2.1. Reagents and apparatus

o-PD, (1S,2S)-PSDO, (1R,2R)-PSDO, drug-free human serum, acetonitrile (ACN), and ethanol (EtOH) were purchased from Sigma–Aldrich (St. Louis, MO, USA). The mixture of 5 mM $Fe(CN)_6^{3-/4-}$ (1:1) in 0.1 M KCl solution was prepared as redox marker in presence of potassium hexacyanoferrate (II), hexacyanoferrate (III) and potassium chloride supplied from Merck. Double distilled water used in all experiments was purified using a Millipore Milli-Q system. The phosphate buffer (PB) at pH 7.4 was used as a supporting electrolyte and stabilizer of the pH of (1S,2S)-PSDO standard solutions in electrochemical analysis. The 10 mM stock solution of (1S,2S)-PSDO was diluted to different concentrations with PB at pH 7.4. All these solutions were kept under refrigerated conditions (at 4 °C).

The electrochemical instrument was used AUTOLAB-PGSTAT100 (Eco Chemie, Utrecht, The Netherlands) running with NOVA 2.1.4 software. The electrochemical cell has consisted of a conventional three-electrode system with platinum wire as the auxiliary electrode, saturated Ag/AgCl (in 3 M KCl, BASi Research Product, USA) as reference electrode, and the bare glassy carbon electrode (GCE) (d = 3 mm, BASi Research Product, USA) as working electrode. Electrochemical measurements of CV and DPV were performed in 0.1 M KCl containing 5 mM $Fe(CN)_6^{3-/4-}$ (1:1) from −0.2 V to 0.8 V at a scanning rate of 50 mV s^{-1}. The pHs of solutions were adjusted by a Mettler-Toledo pH meter (Switzerland). The removal and rebinding process were realized with Thermo-Shaker (Biosan TS-100, Riga, Latvia). For the obtaining of the precision balance, the chemicals were weighed by Ohaus Instruments (Shanghai, China).



Scheme 2. The construction process of the MIP sensor.

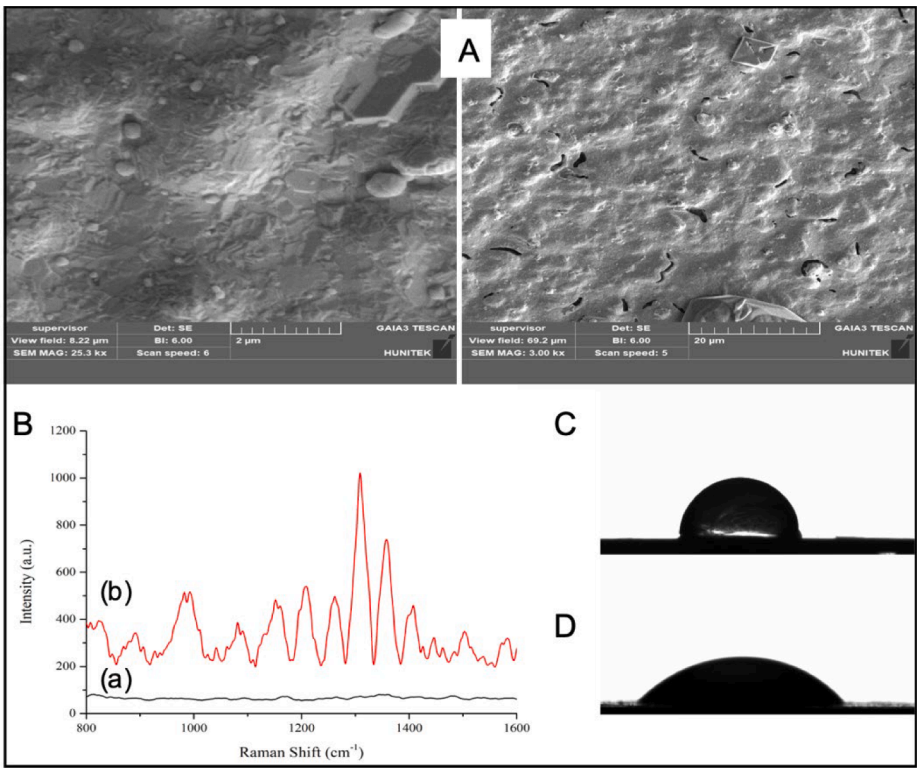


Fig. 1. Characterization of (1S,2S)-PSDO@MIP/GCE surface: SEM image (A); Raman spectra (B); contact angles images of the bare GCE (C); and (1S,2S)-PSDO@MIP/GCE (D).

2.2. GCE-MIP sensor fabrication

The (1S,2S)-PSDO@MIP/GCE was prepared as follows. The bare GC electrode was sonicated in an ultrasonic bath in ethanol:water mixture 1:1 (v:v) before electropolymerization. Next, the surface of the GCE was polished in a 1.0-µm alumina suspension, cleaned with distilled water. For the creation of the MIP sensor, a solution of 1 mM o-PD in phosphate buffer (PB, 0.10 $molL^{-1}$, pH 7.4) and the solution of 1 mM (1S,2S)-PSDO in water were combined at the rate of 1:1 (v:v). Finally, the electropolymerization was applied by CV between −0.2 V and 0.8 V at a scan rate of 50 mV/s with ten scans (Scheme 2).

After electropolymerization of (1S,2S)-PSDO with the functional monomer o-PD on the GCE surface, the (1S,2S)-PSDO@MIP/GCE was rinsed with distilled water. Removal of (1S,2S)-PSDO from the surface, imprinted (1S,2S)-PSDO@MIP/GCE into a solution containing ethanol for 5 min at 350 rpm and 25 °C was performed by immersion using a Thermo-Shaker. Then, for the rebinding of the template, the (1S,2S)-PSDO@MIP/GCE was incubated at different concentrations of (1S,2S)-PSDO for 5 min utilizing a Thermo-Shaker at 350 rpm (25 °C). The (1S,2S)-PSDO@MIP/GCE was rinsed with distilled water in 20 s before immersing in each different concentration.

A non-imprinted sensor (NIP/GCE) was designed using the same procedure except the addition of (1S,2S)-PSDO to realize the control experiments. Electrochemical measurements were performed via DPV, CV, and EIS methods on a NIP/GCE and (1S,2S)-PSDO@MIP/GCE in a solution including 0.1 M KCl and 5 mM $[Fe(CN)_6]^{3-/4-}$ (1:1).

2.3. Characterization studies of (1S,2S)-PSDO@MIP/GCE

The chemical structure of (1S,2S)-PSDO@MIP/GCE sensor was characterized using a confocal Raman microscope (Jasco NRS-4500, Tokyo, Japan) equipped with a 785 nm laser source. The Raman spectra were recorded in the wavenumber range of 800–1600 cm^{-1}. Contact angle (KRUSS DSA100, Hamburg, Germany) of the electrodes was performed to determine the hydrophilicity/hydrophobicity of electrode surface by sessile drop method. The contact angle values were obtained from the average of three values. The morphological structure of (1S,2S)-PSDO@MIP/GCE surface was characterized using scanning electron microscopy (SEM) (TESCAN GAIA 3, Brno–Kohoutovice, Czech Republic).

2.4. Preparation of serum sample and pharmaceutical dosage form

The developed (1S,2S)-PSDO@MIP/GCE sensor was also carried out to determine (1S,2S)-PSDO in a commercial serum sample. For this aim, standard solutions of human commercial serum sample were prepared via mixing 1.0 mL of 10 mM (1S,2S)-PSDO, 5.4 mL of ACN used for the precipitation of protein residuals, and 3.6 mL of the commercial serum sample. Blank serum was prepared with 1.0 mL of 0.1 mM PB pH 7.4, 3.6 mL of a commercial serum sample, and 5.4 mL of ACN. The mixtures were centrifuged for 20 min at 3500 rpm to precipitate protein residues and then the supernatants were collected. An aliquot from the stock mixture of serum was utilized for rebinding of (1S,2S)-PSDO in the electrochemical detection. The desired standard (1S,2S)-PSDO concentration was added to the commercial serum sample. The five consecutive experiments were carried out with the same sensor and solution. The achieved results were evaluated by the relative standard deviation.

Ten effervescent tablets of Deloday Plus® were weighed to form a fine homogeneous powder and crushed in a mortar. A sufficient amount of this powder was weighed, and a 1.0 mM stock solution in distilled water was prepared. Next, this solution was sonicated for about 30 min. Finally, a certain amount of this solution was taken and diluted with PB 7.4 supporting electrolyte solution. For the determination of (1S,2S)-PSDO amount in effervescent tablet samples, calibration data were used. The recovery investigation was performed by adding certain amount of pure (1S,2S)-PSDO and investigated with DPV.

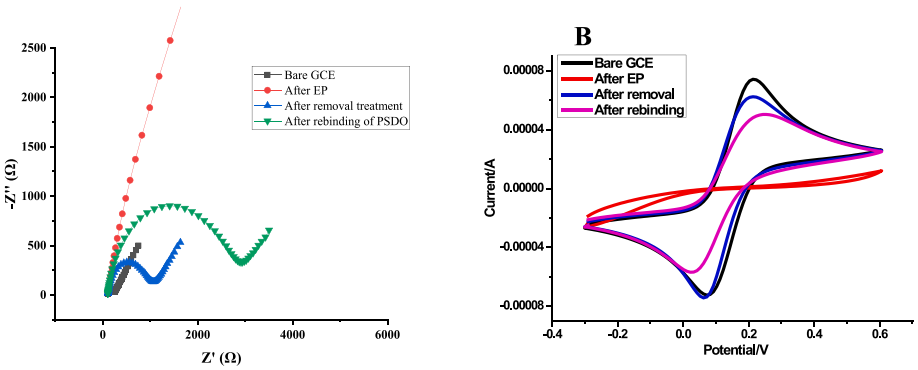


Fig. 2. A) The EIS in each step to form (1S,2S)-PSDO@MIP/GCE sensor B) CV of each step of proposed (1S,2S)-PSDO@MIP/GCE sensor.

2.5. Selectivity studies

Selective recognition ability is most important for the MIP sensor. In this research, the selectivity of (1S,2S)-PSDO@MIP/GCE sensor for (1S,2S)-PSDO was evaluated. (1R,2R)-PSDO, ephedrine and desloratadine were used as competitor molecules due to the similar molecular structure.

3. Results and discussion

3.1. Preparation and characterization of MIP sensor

The (1S,2S)-PSDO@MIP/GCE sensor was designed by o-PD electropolymerization procedure in 0.1 mM PB (pH 7.4) in the presence of template as 1 mM (1S,2S)-PSDO and monomer as 1 mM o-PD in the potential range between −0.2 and 0.8 V at a scan rate of 50 mV s^{-1} by 10 CV scans (Fig. S1). To acquire NIP/GCE, the same process was performed in the absence of a template. A well-defined oxidation peak was achieved at around 0.2 V on GCE, corresponding to the anodic oxidation of the o-PD in Fig. S1. However, this oxidation peak deeply diminished after successive scans of electropolymerization of o-PD due to non-conductive film creation on GCE.

Surface characterization of the (1S,2S)-PSDO@MIP/GCE was investigated using SEM (Fig. 1A). As seen in the figure, (1S,2S)-PSDO imprinted electrode with a uniform coating formed on the surface of GCE. To characterize the chemical structure of (1S,2S)-PSDO@MIP/GCE, we used Raman spectroscopic methods (Fig. 1B). The typical Raman shifts bands were C—N•+ and C═C stretching modes in the benzenoid ring assigned at around 1358 cm^{-1} and 1584 cm^{-1}, respectively. As seen in spectra, the Raman shift at 1502 cm^{-1} corresponds to the C═N stretching vibrations related to imine sites in the sensor surface. The C—N•+stretching vibrations-delocalized polaronic charge carriers were located at 1308 cm^{-1} as a strong Raman band. Also, The C—N stretching vibrations were clearly seen around 1261 cm^{-1}. Contact angle of the bare GCE and (1S,2S)-PSDO@MIP/GCE surface decreased from 72.14° to 35.86° after the sensor fabrication (Fig. 1C, 1D). A significant decrease in contact angle indicated that hydrophilic characters and polarity of the surface increased.

3.2. Electrochemical characterization

In order to examine the electrochemical activity of the proposed MIP-based electrochemical chiral sensors, CV and EIS were used, and the electron transfer properties of the sensor surfaces were investigated in potassium ferricyanide solution, a standard reference redox molecule. They were applied to check results before electropolymerization, after electropolymerization, and after rebinding (1S,2S)-PSDO. EIS is an effective technique for the characterization of sensor procedures and is effective compared with the modified and unmodified electrode surface features. Remarkable EIS alterations in each step were monitored in Fig. 2A. The semi-circle of the Nyquist diagram for higher frequencies corresponds to the electron transfer procedure, while the linear part of the lower frequency corresponds to diffusion. It can be monitored a diffusion-limited procedure with fast electron transfer kinetics for the bare GCE. After electropolymerization, MIP is non-conductive, and the surface was highly insistent to electron transfer. Hence, the maximum insistent impedance spectra were acquired. After removal of (1S,2S)-PSDO, the impedance value diminish due to cavities' creation, and then the signal of $[Fe(CN)_6]^{3-/4-}$ noticed owing to eases the electron transfer electrons. Finally, the semi-circle is improved after the immerse of the (1S,2S)-PSDO. This outcome can be commented as that the polymeric matrix has sufficient capacity to reattach to (1S,2S)-PSDO.

Surface characterization of the proposed sensor was also worked by the CV technique. CV method was applied to assess the electropolymerization, removal, and rebinding procedure. As can be seen in Fig. 2B, bare GCE has the maximum peak current of the $[Fe(CN)_6]^{3-/4-}$. After electropolymerization, the response of $[Fe(CN)_6]^{3-/4-}$ cannot be acquired because of the inhibited electron transfer by polymer development. After the removal of (1S,2S)-PSDO, the $[Fe(CN)_6]^{3-/4-}$ the response was acquired again, showing the formation of cavities permitting rebinding and increased electron transfer. Finally, after rebinding of (1S,2S)-PSDO, a considerable decrease on the $[Fe(CN)_6]^{3-/4-}$ response was obtained because of the reduction of appropriate binding cavities for $[Fe(CN)_6]^{3-/4-}$. (1S,2S)PSDO@MIP/GCE sensor has many benefits in electrochemical chiral sensing areas, such as excellent selectivity and sensitivity and exceptional good reproducibility 0.986 % [28,29].

3.3. Optimization of the experimental conditions

3.3.1. Optimization of monomer/template ratio

The optimization and assessment of the molecular printed film is the most critical phase of MIP-based sensor design. By optimizing the monomer to template molar ratio, suitable bonding spaces and stable and homogeneous polymer creation can be achieved. For this reason, the monomer to template molar ratio was examined as 0.5:1, 1:1, 2.5:1, 5:1, and 10:1 (Fig. 3A). The DPV and CV responses of the developed sensors at different rates were checked before electropolymerization, after electropolymerization, removal, and rebinding. Consequently, the monomer/template molar ratio was found 1:1 to provide an easy removal process, good stability, and efficient rebinding process and was chosen as the optimum ratio.

3.3.2. Effect of number of cycles and scan rate for electropolymerization

One of the most critical processes affecting the polymer film thickness and the performance of the enhanced printed sensor, such as selectivity, stability, and sensitivity, is the number of cycles. Therefore, 3, 5, 10, 15, and 20 cycles were performed during electropolymerization to compare the influence of cycle numbers. To acquire a more accurate assessment, the difference between peak currents (Ip) measurement

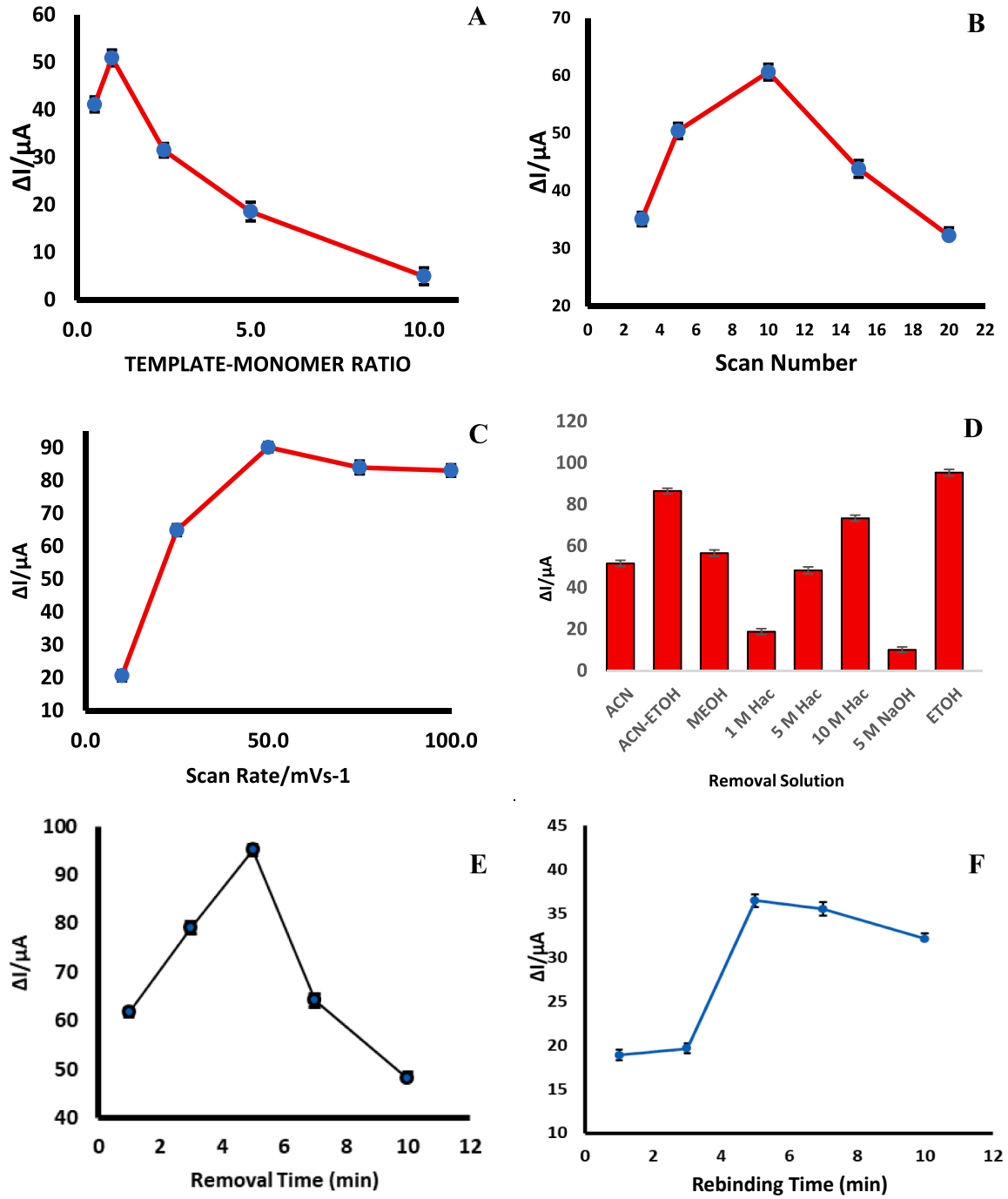


Fig. 3. A) Optimization of monomer/template ratio, scan number (B) and scan rate (C). Effect of removal solutions (D) and removal times (E) with the plot of ΔIp values after removal and after rebinding of $5x10^{-15}$ M (1S,2S)-PSDO. The plot of ΔIp values after removal and after rebinding of $5x10^{-15}$ M (1S,2S)-PSDO versus different rebinding times (F).

after removal of the (1S,2S)-PSDO and after rebinding of $5x10^{-15}$ M (1S,2S)-PSDO (ΔIp) was checked out. According to the acquired results, 10 cycles (Fig. 3A) were selected as the best convenient for electropolymerization. While determining the potential scanning rate, electropolymerizations were carried out at potential scanning rates of 10, 25, 50, 75 and 100 mV/s by keeping the potential scanning range of −0.2–0.8 V and the number of cycles constant at 10. According to the results obtained, it was decided that the most suitable scanning speed for electropolymerization was 50 mV/s (Fig. 3C). In addition, when the potential scanning rate was further increased, the difference between the observed peak currents decreased when the polymer films were electropolymerized.

3.3.3. *Template removing treatment*

Another critical parameter for optimizing the sensor is a smooth extraction. The removal solution and time selection should be optimized to achieve adequate removal without damaging the polymer film. Firstly, different removal solutions such as ACN, ACN:EtOH (1:1), methanol, acetic acid (1, 5, and 10 M), 5 M NaOH, and EtOH were used. EtOH provided efficient removal of (1S,2S)-PSDO compared to other solutions and consequently was used as a removal solution in later studies (Fig. 3D). Afterward, a convenient time for incubating the developed sensor into the EtOH was optimized. The (1S,2S)-PSDO@-MIP/GCE was incubated into EtOH for 1, 3, 5, 7, and 10 min was utilizing a Thermo Shaker (350 rpm, 25 °C). After rebinding $5x10^{-15}$ M

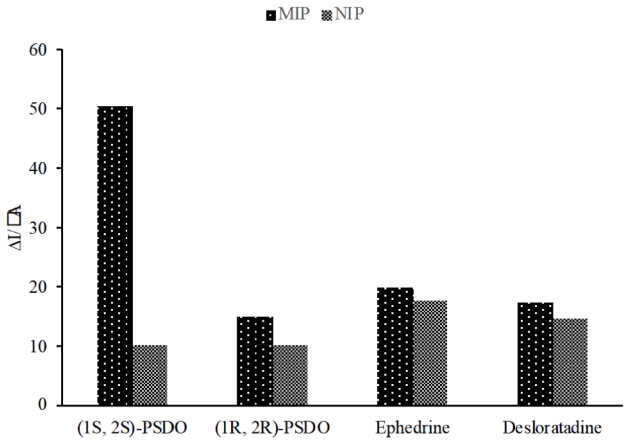


Fig. 4. The evaluation of IF values for (1S,2S)-PSDO, (1R,2R)-PSDO, Ephedrine, and Desloratadin.

(1S,2S)-PSDO for 5 min, ΔIp values were checked at different times (Fig. 3E). As the removal time raised, the response of the (1S,2S)-PSDO@MIP/GCE also increased similarly. (1S,2S)-PSDO were progressively removed from the polymer matrix. Five minutes later, the peak response decreases, which explains the over swelling of the polymer, and so can lead to clogging of the voids. In the end, the optimal time for removal process was found to be 5 min.

3.3.4. Optimization of incubation time

Another important parameter in MIP-based sensors is optimizing the incubation time, related to the detection time and analytical efficiency of the sensor. 1, 3, 5, 7, and 10 min were examined by incubating $5x10^{-15}$ M (1S,2S)-PSDO to test the effect of the incubation time, and using a Thermo Shaker at 350 rpm and 25 °C. As seen in Fig. 3F, ΔIp values increase up to 5 min. After 5 min, ΔIp decreased continuously. This shows that the incubation time of 5 min provides the optimal reattachment time for (1S,2S)-PSDO. While the rebinding ability and affinity of MIP cavities were not enough at shorter incubation times, longer incubation times resulted in decreased sensor efficiency.

3.4. Imprinting factor

The selectivity of (1S,2S)-PSDO@MIP/GCE was assessed by the response of the similar compound structure of (1S,2S)-PSDO. The signal of (1S,2S)-PSDO@MIP/GCE was checked with DPV result using $5x10^{-15}$ M amount of similar compounds such as (1R,2R)-PSDO, Ephedrine, and Desloratadine (Fig. 4).

The selectivity of the proposed sensor was investigated with the imprinting factor (IF). It is described as the rate of the imprinting (ΔI (MIP)) to non-imprinting (ΔI(NIP)) electrode peak signal using the following equation:

$$IF = \Delta I(MIP)/\Delta I(NIP)$$

Herein, ΔI = Io - I, where Io and I are the peak signals of the designed electrode in the removal and rebinding of (1S,2S)-PSDO, respectively. The obtained IFs for the (1S,2S)-PSDO@MIP/GCE was 4.97, 1.51, 1.11, and 1.19 for (1S,2S)-PSDO, (1R,2R)-PSDO, Ephedrine, and Desloratadin, respectively. These outcomes proved that the (1S,2S)-PSDO@MIP/GCE could bind selectively with (1S,2S)-PSDO compounds.

3.5. Interference analysis

For the investigation of the interference effect, the analysis was carried out by adding some potential interference materials to the analysis environment. Biologically important substances such as ascorbic acid (AA), dopamine (DOP), uric acid (UA), paracetamol (PAR), and

Table 1
Effect of interfering agents on the detection of (1S,2S)-PSDO.

Interference agents	I = Im/Io	RSD (%)
UA	101.98	0.96
DOP	100.32	0.66
PAR	100.37	0.63
AA	99.74	0.58
Na^+	100.55	0.49
SO_4^{2-}	99.63	0.42

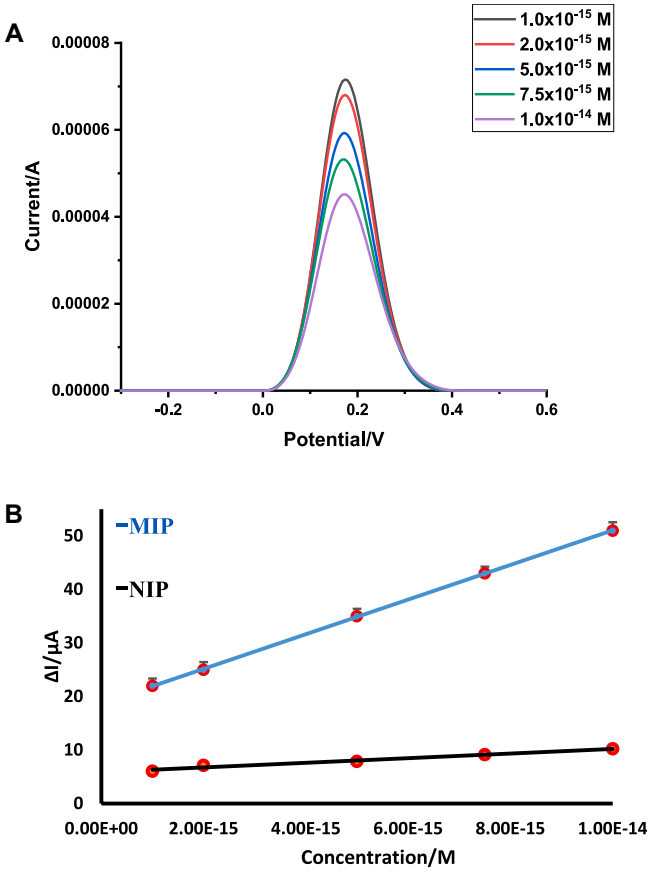


Fig. 5. DPV of (1S,2S)-PSDO on the (1S,2S)-PSDO@MIP/GCE (A) A linear relationship between the ΔI and (1S,2S)-PSDO concentrations in (1S,2S)-PSDO@MIP/GCE and NIP/GCE (B).

cationic and anionic substances such as Na^+, and SO_4^{2-} were determined as potential interference materials. I = Im/Io and RSD (%) values were calculated by mixing the ingredients showing interference influence with (1S, 2S)-PSDO at a rate of 1:10. As given in Table 1, relative error values were acquired between 99.63 % and 101.98 %. The obtained results showed that the proposed (1S,2S)-PSDO@MIP/GCE sensor could be applied close to the peak signal in the presence of interference agents.

3.6. Electrochemical recognition of pseudoephedrine enantiomers

The analytical curve of (1S,2S)-PSDO assessed the analytical efficiency of the (1S,2S)-PSDO@MIP/GCE. After incubation of different concentrations of (1S,2S)-PSDO, the peak signal of the (1S,2S)-PSDO@MIP/GCE was acquired utilizing the current of the anodic peak at 0.16 V related to the $[Fe(CN)_6]^{3-/4-}$.

A linear relationship between the ΔI and (1S,2S)-PSDO concentrations was observed between $1.0x10^{-15}$ – $1.0x10^{-14}$ M, which showed the following linear regression equation: $\Delta I = 3x10^{15}$ [(1S,2S)-PSDO] + 20.219, ($R^2 = 0.996$) (Fig. 5).

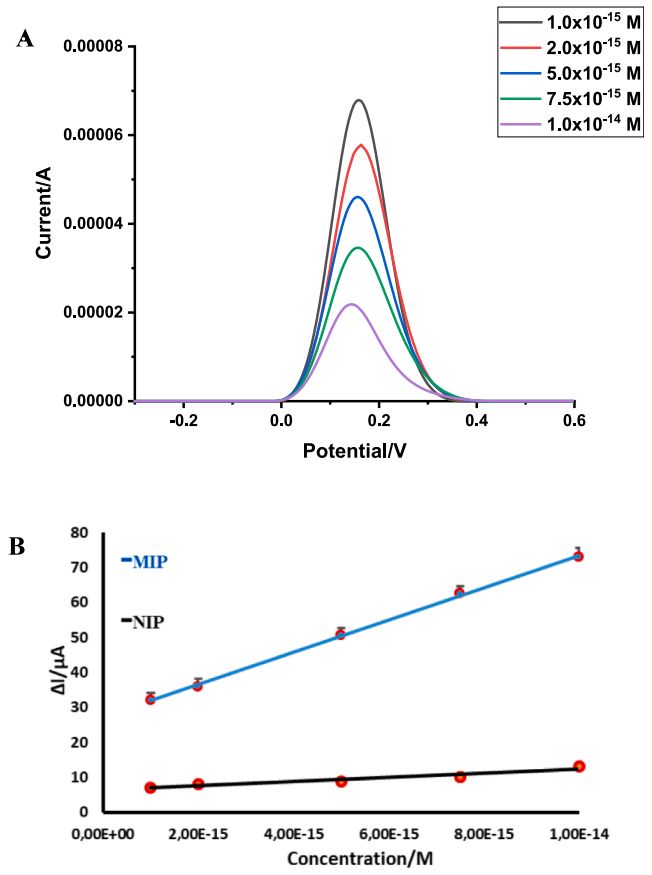


Fig. 6. In spiked serum samples, DPV of (1S,2S)-PSDO on the (1S,2S)-PSDO@MIP/GCE (A) and A linear relationship between the ΔI and (1S,2S)-PSDO concentrations in (1S,2S)-PSDO@MIP/GCE and NIP/GCE (B).

Table 2
Regression data of the calibration lines for detection of (1S,2S)-PSDO by DPV in standard solution and serum sample.

Parameter	Standard solution	Serum
Linearity range (M)	$1x10^{-15}$ – $1x10^{-14}$	$1x10^{-15}$ – $1x10^{-14}$
Slope (μA/M)	$2.98x10^{15}$	$2.13x10^{15}$
SE of slope	0.346	0.402
Intercept (μA)	20.637	76.502
SE of intercept	6.534	9.16
Correlation coefficient (*r*)	0.998	0.998
LOD (M)	$2.98x10^{-16}$	$3.01x10^{-16}$
LOQ (M)	$9.84x10^{-16}$	$9.97x10^{-16}$
Repeatability of peak current (RSD%)[a]	0.648	0.593
Reproducibility of peak current (RSD %)[a]	0.986	0.947

[a] Each value is the mean of five experiments.

LOD and LOQ are calculated using the slope value of the calibration equation and the standard deviation obtained from at least 5 measurement results of the response of the analyte at the lowest concentration in the calibration curve. LOD and LOQ were found at $2.98x10^{-16}$ M and $9.84x10^{-16}$ M, respectively [28,29].

The DPV of rebinding of different concentrations of on the (1S,2S)-PSDO 1S,2S)-PSDO@MIP/GCE was shown in Fig. 6. The DPV peak current was reduced due to the occupation of specific cavities with (1S,2S)-PSDO compounds when a higher concentration of (1S,2S)-PSDO was rebinding.

The NIP was used for the comparison of the developed (1S,2S)-PSDO@MIP/GCE sensor. As seen in Fig. 6, the ΔI results stay nearly unaffected when the various amounts of (1S,2S)-PSDO were rebinding, which the non-retention of the (1S,2S)-PSDO can comment.

Table 3
Results of Deloday Plus® effervescent tablets and the serum samples experiments for the (1S,2S)-PSDO analysis.

	Deloday Plus ®	Serum
Label amount (mg)	60.00	–
Found amount (mg)	60.4	–
RSD%[a]	1.10	–
Bias%	0.67	–
Added amount (mg)	20.00	5.00
Found amount (mg)	20.10	5.02
Average recovery (%)	100.50	100.40
RSD% of recovery[a]	0.78	0.46
Bias%	0.50	0.40

[a] Each value is the mean of five experiments.

Table 4
Recent electrochemical studies about Pseudoephedrine.

Sensor	Method	Linear range	LOD	Ref.
Multi-walled carbon nanotubes (MWCNTs)-GCE	Adsorptive stripping voltammetry (AdSV)	1–100 μM	0.82 μM	[14]
Ni – Co@Pt/C – 3	DPV	–	4.17 μM	[30]
PVC membrane electrode	Potentiometric	10^{-5}–10^{-6} M	9.00 μM	[31]
Mn@Pt/C	Chronoamperometry	5–1400 μM	1.72 μM	[32]
(1S,2S)-PSDO@MIP/GCE	DPV	$1x10^{-15}$ – $1x10^{-14}$ M	$2.98x10^{-16}$ M	This work

3.7. Analysis of (1S,2S)-PSDO in pharmaceutical dosage forms and serum samples

The analytical performances of the proposed (1S,2S)-PSDO@MIP/GCE sensor were showed by practice to effervescent tablets and commercial serum samples. As seen in Table 2, the great linearity between Ip and C was found with LODs $9.97x10^{-16}$ M and (1S,2S)-PSDO recovery values. As seen in Fig. 5, the practical benefit of the (1S,2S)-PSDO@MIP/GCE and NIP/GCE was performed by defining the concentration of (1S,2S)-PSDO using the standard addition technique in commercial human serum samples. The (1S,2S)-PSDO@MIP/GCE and NIP/GCE were immersed with commercial serum samples with varied (1S,2S)-PSDO solutions from $1x10^{-15}$ – $1x10^{-14}$ M.

As seen in Table 3, the 101.46 % and 101.2 % recovery values were obtained with 1.62 % and 1.26 % relative standard deviation values in effervescent tablets and commercial serum samples, respectively. The stability of the developed sensor was investigated by measuring the current response of the sensor with $1x10^{-15}$ M (1S,2S)-PSDO during the day. The stability of the developed sensor was found to be 1 day. Recent electrochemical studies about Pseudoephedrine added in Table 4.

4. Conclusion

In this study, (1S,2S)-PSDO imprinted GCE was investigated for determination of (1S,2S)-PSDO in effervescent tablets and commercial serum samples for the first time. The proposed sensor was prepared with electropolymerization of o-PD monomer in the presence of (1S,2S)-PSDO. Each step was monitored with a redox marker using CV and DPV techniques. The fabricated sensor platform offered a fast, economical, and environmental-friendly system for the electrochemical detection of

(1S,2S)-PSDO. Furthermore, (1S,2S)-PSDO@MIP/GCE sensor represents a very low LOD with $2.98x10^{-16}$ M and $3.01x10^{-16}$ for standard solution and commercial serum sample, respectively. In addition, the designed sensor platform displayed highly selective and effective for (1S,2S)-PSDO detection compared with other competitor agents. Hence, the proposed MIP sensor has a great potential to be applied in a pharmaceutical area as an alternative tool.

CRediT authorship contribution statement

Leyla Karadurmus: Investigation, Conceptualization, Writing – original draft. **Goksu Ozcelikay:** Investigation, Conceptualization, Writing – original draft. **Canan Armutcu:** Conceptualization, Writing – review & editing. **Sibel A. Ozkan:** Supervision, Conceptualization, Writing – review & editing.

Declaration of Competing Interest

The authors declare that they have no known competing financial interests or personal relationships that could have appeared to influence the work reported in this paper.

Acknowledgements

This work is produced from PhD Thesis of Leyla Karadurmus (Ankara University, Health Science Institute).

Appendix A. Supplementary data

Supplementary data to this article can be found online at https://doi.org/10.1016/j.microc.2022.107820.

References

[1] H. Brown, K.A. Pollard, Drugs of abuse sympathomimetics, Crit. Care Clin. 37 (3) (2021) 487–499.
[2] K. Głowacka, A. Wiela-Hojé, S. Komarnytsky, A. Matkowski, Molecular Sciences Pseudoephedrine-Benefits and Risks (2021), https://doi.org/10.3390/ijms22105146.
[3] J. Cristina, M. Elizabeth, Q. Bezerra, Challenges and innovations in chiral drugs in an environmental and bioanalysis perspective, Trends Anal. Chem. 142 (2021), 116326, https://doi.org/10.1016/j.trac.2021.116326.
[4] B. Swanson-Biearman, Pseudoephedrine, Encycl. Toxicol. (2005) 556–557. https://doi.org/10.1016/B0-12-369400-0/00811-5.
[5] L. Prisco, A. Sarwal, M. Ganau, F. Rubulotta, Toxicology of psychoactive substances, Toxicology of Psychoactive Substances 37 (3) (2021) 517–541.
[6] Wold-Anti Doping Agency (WADA), Prohibited List 2022, World Anti-Doping. (2016) 1–116.
[7] M.A. Fravel, M. Ernst, Drug interactions with antihypertensives, Curr. Hypertens. Rep. 23 (2021) 1–8, https://doi.org/10.1007/s11906-021-01131-y.
[8] WADA, World Anti-Doping Code International Standard: The WADA Prohibited List World Anti-Doping. 2021 2021 1 24 https://www.wada-ama.org/sites/default/files/resources/files/2021list_en.pdf.
[9] A. Pokrywka, W. Tszyrsznic, D.J. Kwiatkowska, Problems of the use of pseudoephedrine by athletes, Int. J. Sports Med. 30 (2009) 569–572, https://doi.org/10.1055/s-0029-1202826.
[10] E.A. Khudaish, A. Al-Khodouri, A surface network based on reduced graphene oxide/gold nanoparticles for selective determination of norepinephrine in real samples, J. Electrochem. Soc. 167 (2020), 146516, https://doi.org/10.1149/1945-7111/ABC5DB.
[11] E. Mazzotta, R.A. Picca, C. Malitesta, S.A. Piletsky, E.V. Piletska, Development of a sensor prepared by entrapment of MIP particles in electrosynthesised polymer films for electrochemical detection of ephedrine, Biosens. Bioelectron. 23 (2008) 1152–1156, https://doi.org/10.1016/j.bios.2007.09.020.
[12] I. Aldama, V. Barranco, J. Ibañez, J.M. Amarilla, J.M. Rojo, A procedure for evaluating the capacity associated with battery-type electrode and supercapacitor-type one in composite electrodes, J. Electrochem. Soc. 165 (2018) A4034–A4040, https://doi.org/10.1149/2.1131816jes.
[13] J.R. González Lomba, E. Pinilla Gil, P. Cintas Moreno, R.M. García-Moncó Carra, A. Sánchez Misiego, Anodic oxidation of thioureido derivatives of biogenic amines at a glassy carbon electrode in an aqueous medium, J. Electroanal. Chem. 410 (1996) 87–92, https://doi.org/10.1016/0022-0728(96)04550-0.
[14] H. Ahmar, A.R. Fakhari, Electro-oxidation and adsorptive stripping voltammetric determination of ephedrine and pseudoephedrine at carboxylated multi-walled carbon nanotube-modified electrode, Anal. Methods. 4 (2012) 812–818, https://doi.org/10.1039/c2ay05680a.
[15] R.M. Abdel Hameed, A core-shell structured Ni-Co@Pt/C nanocomposite-modified sensor for the voltammetric determination of pseudoephedrine HCl, New J. Chem. 42 (2018) 2658–2668, https://doi.org/10.1039/c7nj04973k.
[16] Y.K. Dijiba, T.M. Niemczyk, Determination of ephedrine hydrochloride in mixtures of ephedrine hydrochloride and pseudoephedrine hydrochloride using near infrared spectroscopy 160 (2005) 155–160.
[17] W. Wang, C. Li, Y. Li, Z. Hu, X. Chen, Rapid and ultrasensitive determination of ephedrine and pseudoephedrine by micellar electrokinetic chromatography with laser-induced fluorescence detection 1102 (2006) 273–279, https://doi.org/10.1016/j.chroma.2005.10.015.
[18] E. Marchei, M. Pellegrini, R. Pacifici, P. Zuccaro, S. Pichini, A rapid and simple procedure for the determination of ephedrine alkaloids in dietary supplements by gas chromatography – mass spectrometry 41 (5) (2006) 1633–1641.
[19] P. Van Eenoo, F.T. Delbeke, K. Roels, P. De Backer, Simultaneous quantitation of ephedrines in urine by gas chromatography-nitrogen-phosphorus detection for doping control purposes, J. Chromatogr. B Biomed. Sci. Appl. 760 (2001) 255–261, https://doi.org/10.1016/S0378-4347(01)00275-4.
[20] M. Review, Y. Sun, S. Zhang, Application of Capillary Electrophoresis for Ephedrine and Pseudoephedrine Detection : a Review 15 (2020) 2614–2623. https://doi.org/10.20964/2020.03.38.
[21] S.A. Piletsky, A.P.F. Turner, Electrochemical sensors based on molecularly imprinted polymers, Electroanalysis 14 (2002) 317–323, https://doi.org/10.1002/1521-4109(200203)14:5<317::AID-ELAN317>3.0.CO;2-5.
[22] L. Karadurmus, M.E. Corman, L. Uzun, S.A. Ozkan, Enantioselective recognition of esomeprazole with a molecularly imprinted sol-gel-based electrochemical sensor, Mikrochim. Acta. 189 (2022) 225, https://doi.org/10.1007/S00604-022-05321-6.
[23] A. Cetinkaya, S.I. Kaya, M.E. Çorman, M. Karakaya, E. Bellur Atici, S.A. Ozkan, A highly sensitive and selective electrochemical sensor based on computer-aided design of molecularly imprinted polymer for the determination of leflunomide, Microchem. J. 179 (2022), 107496, https://doi.org/10.1016/J.MICROC.2022.107496.
[24] M.E. Çorman, A. Cetinkaya, G. Ozcelikay, E. Özgür, E.B. Atici, L. Uzun, S.A. Ozkan, A porous molecularly imprinted nanofilm for selective and sensitive sensing of an anticancer drug ruxolitinib, Anal. Chim. Acta. 1187 (2021), 339143, https://doi.org/10.1016/J.ACA.2021.339143.
[25] X. Zheng, S. Khaoulani, N. Ktari, M. Lo, A.M. Khalil, C. Zerrouki, N. Fourati, M. M. Chehimi, Towards clean and safe water: A review on the emerging role of imprinted polymer-based electrochemical sensors, Towards Clean and Safe Water: A Review on the Emerging Role of Imprinted Polymer-Based Electrochemical Sensors 21 (13) (2021) 4300.
[26] P. Rebelo, E. Costa-Rama, I. Seguro, J.G. Pacheco, H.P.A. Nouws, M.N.D. S. Cordeiro, C. Delerue-Matos, Molecularly imprinted polymer-based electrochemical sensors for environmental analysis, Biosens. Bioelectron. 172 (2021), 112719, https://doi.org/10.1016/J.BIOS.2020.112719.
[27] L. Chen, X. Wang, W. Lu, X. Wu, J. Li, Molecular imprinting: perspectives and applications, Chem. Soc. Rev. 45 (2016) 2137–2211, https://doi.org/10.1039/c6cs00061d.
[28] S.A. Ozkan, J.-M. Kauffmann, P. Zuman, Electroanalytical Method Validationmethod validation in Pharmaceutical Analysis and Their Applications, in: Springer, Berlin, Heidelberg, 2015: pp. 235–266. https://doi.org/10.1007/978-3-662-47138-8_8.
[29] Ich Harmonised Tripartite Guideline, Guidance for Industry Q2B Validation of Analytical Procedures: Methodology, 20857 (1996) 301–827.
[30] R.M. Abdel Hameed, A core–shell structured Ni–Co@Pt/C nanocomposite-modified sensor for the voltammetric determination of pseudoephedrine HCl, New J. Chem. 42 (2018) 2658–2668, https://doi.org/10.1039/C7NJ04973K.
[31] M.R. Ganjali, A. Alipour, S. Riahi, B. Larijani, P. Norouzi, Quantitative Analysis of Pseudoephedrine in Formulation by Potentiometric Membrane Sensor; Computational Investigation, Int. J. Electrochem. Sci. 4 (2009) 1262–1276. www.electrochemsci.org (accessed May 25, 2022).
[32] R.M.A. Hameed, Influence of incorporating manganese in Pt/C on its electrochemical performance towards pseudoephedrine HCl assaying, Colloids Surfaces A Physicochem. Eng. Asp. 570 (2019) 11–21, https://doi.org/10.1016/J.COLSURFA.2019.03.008.